

# Efficient Design of Inline E-Plane Waveguide Extracted Pole Filters Through Enhanced Equivalent Circuits and Space Mapping

Oleksandr Glubokov, Slawomir Koziel and Leifur Leifsson

**Abstract** A design procedure for inline waveguide extracted pole filters with all-metal E-plane inserts is presented. To achieve acceptable modeling accuracy for this class of filters, an enhanced schematic-circuit-based surrogate model is developed, accounting for parasitic effects between the neighboring elements of the structure. The proposed circuit representation is used as a coarse model in a surrogate-based optimization of the filter structure with the space mapping technique as the main engine in the optimization process. Feasibility of the modeling approach is demonstrated by two filter design examples. The examples show that a low computational cost (corresponding to a few evaluations of the high-fidelity EM simulations of the filter structure) is required to obtain an optimized design.

**Keywords** Inline filters · E-plane filters · Extracted pole filters · Waveguide · Modeling · Surrogate optimization

## 1 Introduction

Filters based on rectangular waveguide structures have been one of the most popular solutions for frequency selection in microwave and millimeter-wave systems in the past decades. However, massive housings, typically used for implementation of the waveguide structures, make them less attractive for specific applications such as satellite communications. It is, therefore, highly desirable to

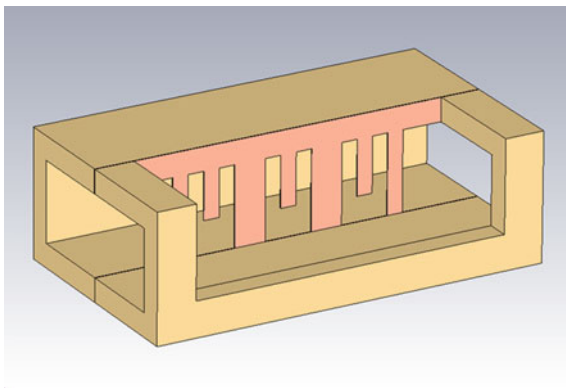
---

O. Glubokov · S. Koziel (✉) · L. Leifsson  
Engineering Optimization and Modeling Center, School of Science and Engineering,  
Reykjavik University, Menntavegur 1, Reykjavik 101, Iceland  
e-mail: koziel@ru.is

O. Glubokov  
e-mail: oleksandr@ru.is

L. Leifsson  
e-mail: leifurth@ru.is

**Fig. 1** Configuration of an inline E-plane waveguide extracted pole filter



miniaturize the components. This can be achieved by using an extracted pole filters concept. Inline E-plane extracted pole filters, which are cheap and easy-to-fabricate, allow for designing the devices with the required compactness, as well as preserving their filtering properties. Miniaturized inline E-plane extracted pole filters with high stopband performance using standard and enhanced extracted pole sections have been previously reported in [7, 8]. In [7], a generalized coupling coefficients extraction procedure is developed, allowing one to obtain a good initial design for this type of filters. However, further optimization of the filter structures is usually time consuming, as numerous analyses of densely meshed objects in full wave simulators are required. Surrogate-based optimization (SBO) offers a way to reduce the number of the required high-fidelity EM simulations [10].

The inline E-plane filters consist of several extracted pole sections containing touching and non-touching axial and transversal strips arranged within a rectangular waveguide, as shown in Fig. 1. Chang and Khan [3] have proposed equation-based surrogate models for these elements. Unfortunately, the model of the non-touching strip is not available in commonly used circuit simulators (e.g., Agilent ADS, [1]) as a component. At the same time, an explicit equation is only available for the transversally coupled strips [4], while couplings between the elements have a significant impact on the performance of the entire filter.

This chapter describes equation-based surrogate models for the touching and non-touching strips placed in the rectangular waveguide's E-plane. A surrogate circuit model of the filter is composed of the models where the coupling between adjacent strips are accounted for by tuning elements. The circuit model is subsequently used in an SBO scheme where space mapping [2, 9] is used as the optimization algorithm with a suitably corrected circuit model utilized as the surrogate. We demonstrate that the SBO approach allows us to achieve the optimal design at a low computation cost corresponding to a few high-fidelity EM simulations of the structures of interest using 2nd- and 4th-order EPS filter examples.

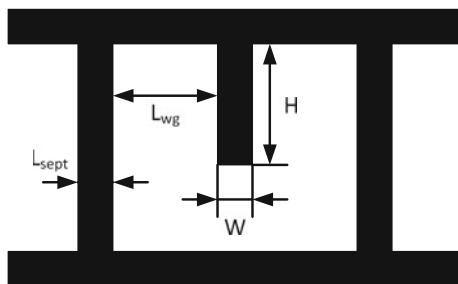


Fig. 2 E-plane waveguide insert with a resonating fin implementing an extracted pole section

## 2 Extracted Pole Section's Model

A single extracted pole section (EPS) can be implemented by an insert (here, all-metal) placed within the E-plane of a rectangular waveguide. The insert, shown in Fig. 2, consists of two strips connecting top and bottom ground planes (input/output septa) and a strip connected to the top ground plane with the other end left open (resonating fin); the septa and the fin are connected in series through uniform waveguide sections.

The EPS is capable of producing a single transmission zero at the fin's resonant frequency and up to two poles depending on the lengths of the waveguide sections  $L_{wg}$ . If  $L_{wg} < \lambda_g/2$ , the transmission zero appears above a single pole. In this case inductive and capacitive couplings between the fin and the septa are non-negligible and strongly affect the positions of the pole and zero, especially for small  $L_{wg}$ . The couplings may be neglected in the case of  $L_{wg} \approx \lambda_g/2$ , when two closely located poles can be obtained with the transmission zero located on either side of them, or even between the poles.

In order to create a surrogate model, the EPS is decomposed into septa, fin and waveguide sections. The septa and the fin are represented as circuit models; next, we compose the EPS of the developed models, and add tuning elements to the obtained circuit in order to take into account the couplings between the septa and the fin. The details are provided in the following subsections.

### 2.1 Septum Model

The circuit model of the septum is shown in Fig. 3. It contains four parameters: two inductances  $L_{s1}$  and  $L_{s2}$ , a capacitance  $C_s$  and a coupling coefficient  $k_s$ . It is implied for all the modeled structures in this paper that the waveguide is air-filled and its parameters, height and width, are kept constant for the design; therefore the septum's model parameters depend on the design parameter  $L_{sept}$  only.

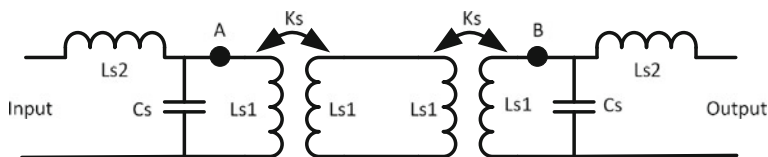


**Fig. 3** Circuit model of the septum

Initial experiments indicate that the following set of equations is suitable to approximate the dependence of the model parameters on  $L_{sept}$  (denoted here as  $x$  in the interest of better readability):

$$L_{s1} = a_{L_{s1}}e^{-b_{L_{s1}}x} + c_{L_{s1}}e^{-d_{L_{s1}}x} \tag{1a}$$

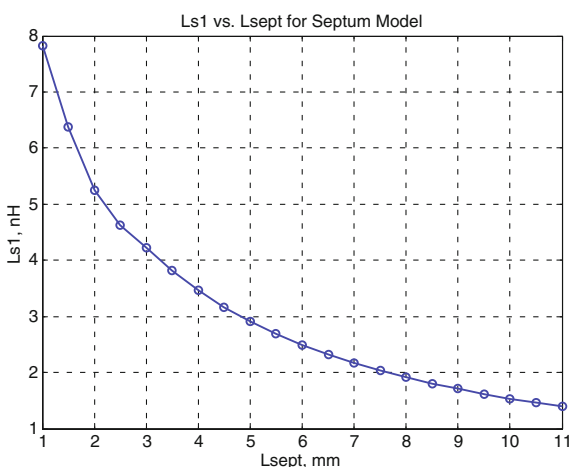
$$L_{s2} = a_{L_{s2}}x^2 + b_{L_{s2}}x + c_{L_{s2}} \tag{1b}$$

$$C_s = a_{C_s}e^{-b_{C_s}x} + c_{C_s}e^{-d_{C_s}x} \tag{1c}$$

$$K_s = a_{K_s}x^2 + b_{K_s}x + c_{K_s} \tag{1d}$$

In order to extract the model parameters, high-fidelity models of the septa are built and analyzed in CST Microwave Studio™ for  $L_{sept} = 1 \dots 11$  mm. The real and imaginary parts of the S-parameters of the proposed circuit model are subsequently fitted to the ones obtained from simulations using the least squares criterion within the frequency range 8...14 GHz. The extraction is illustrated in Fig. 4, where one of the model parameters  $L_{s1}$  is plotted against the design parameter  $L_{sept}$ .

**Fig. 4** Extracted value of  $L_{s1}$  as a function of the design parameter  $L_{sept}$



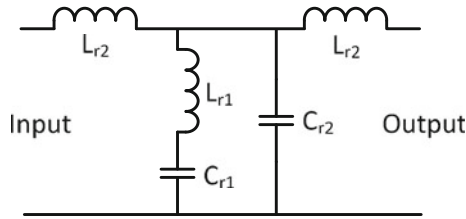


Fig. 5 Circuit model of the resonating fin

### 2.2 Resonating Fin Model

Figure 5 presents a circuit model of the resonating fin. Similarly to the previously considered model of the septum, this one also contains four model parameters: two inductances  $L_{r1}$  and  $L_{r2}$ , and two capacitances  $C_{r1}$  and  $C_{r2}$ . The resonating fin has two design parameters: height  $H$  and width  $W$ . The range of variation of the design parameters is determined based on the assumption that the transmission zeros are located within the frequency range of 8...14 GHz; this condition is sufficient for all the variety of filter design problems that can be solved by the structures under consideration. Consequently, the resonating fin model is created for  $H = 4.5...9.5$  mm and  $W = 1...6$  mm.

Following the investigation of the relationship between the design and model parameters, it has been determined that the best fit can be obtained by using the set of equations:

$$L_{r1} = (e^{a_{Lr1}H} + e^{b_{Lr1}W}) \left[ c_{Lr1} \left( \frac{H}{W} \right)^2 + d_{Lr1} \frac{H}{W} + f_{Lr1} \right] \tag{2a}$$

$$L_{r2} = a_{Lr2}HW + b_{Lr2}H + c_{Lr2}W + d_{Lr2} \tag{2b}$$

$$C_{r1} = (e^{a_{Cr1}H} + e^{b_{Cr1}W}) \left[ c_{Lr1} \frac{H}{W} + d_{Lr1} \right] \tag{2c}$$

$$C_{r2} = a_{Cr2}H^2 + b_{Cr2}HW + c_{Cr2}H + d_{Cr2}W + f_{Cr2} \tag{2d}$$

Extraction of the fin model parameters has also been carried out by fitting the real and imaginary parts of the S-parameters of the circuit model to the ones simulated in CST Microwave Studio™. Typical results of the fin modeling procedure are demonstrated in Figs. 6 and 7.

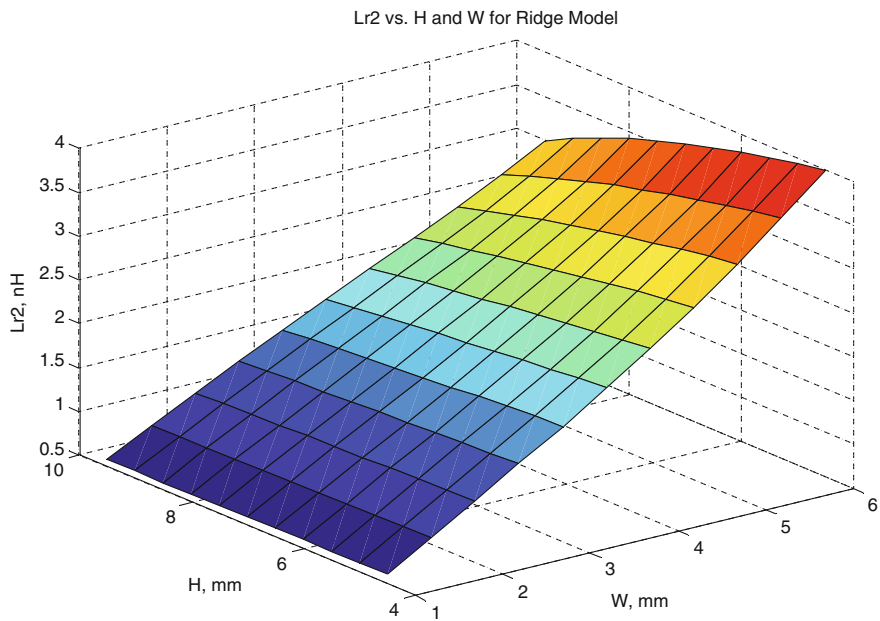


Fig. 6 Extracted value of  $L_{r2}$  as a function of height  $H$  and width  $W$  of the resonating fin

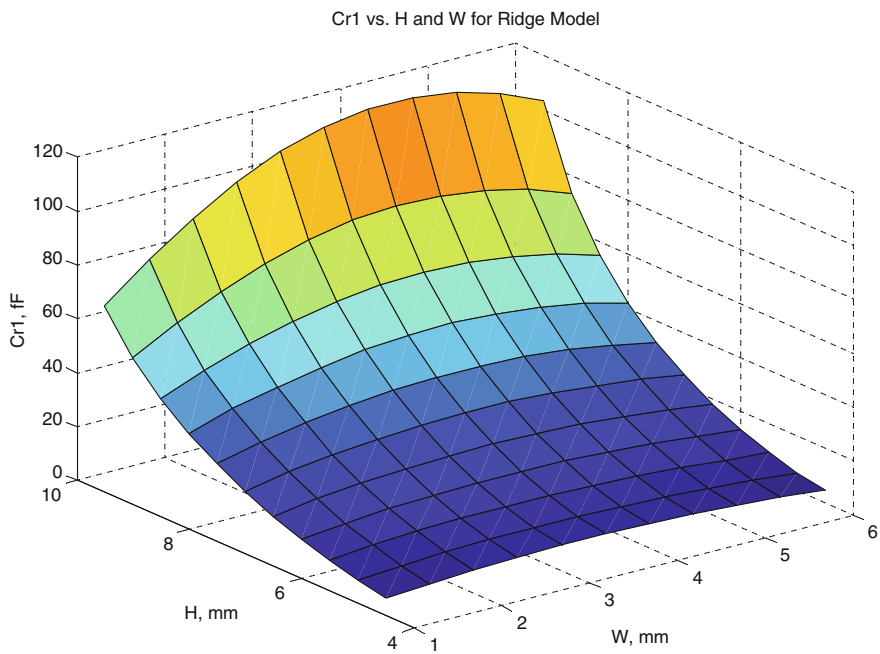


Fig. 7 Extracted value of  $C_{r1}$  with respect to the height  $H$  and width  $W$  of the resonating fin

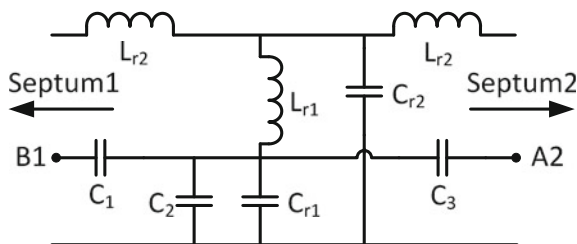


Fig. 8 Model of the capacitive coupling between septa and a fin

### 2.3 Couplings Model

In order to achieve better upper stopband performance of the filter one needs to place transmission zeros as close as possible to the filter's passband. In the inline E-plane waveguide filter this can be made by decreasing the lengths of the waveguide sections  $L_{wg}$ . On this condition, parasitic inductive and capacitive couplings between the adjacent elements significantly affect the frequency responses: poles and zeros drift to the new positions. Therefore, coupling effects between the septa and the resonating fins should be taken into account in the circuit model. In the model, we arrange the inductive coupling by the magnetic coupling coefficient  $K_{sr}$  introduced between the inductors  $L_{s1}$  and  $L_{r1}$ . At the same time, we take the capacitive coupling into consideration by adding three capacitors  $C_1$ ,  $C_2$  and  $C_3$ , as shown in Fig. 8.

$$K_{sr,i} \approx k_i H_i / L_{wg,i} \quad (3a)$$

$$C_{1,i} \approx c_{1i} L_{sept,i} / L_{wg,i} \quad (3b)$$

$$C_{2i} \approx c_{2i} H_i / L_{wg,i} \quad (3c)$$

$$C_{3i} \approx c_{3i} L_{sept,i+1} / L_{wg,i} \quad (3d)$$

## 3 Filter Optimization

The optimization procedure adopts the implicit space mapping technique [5]. Let us denote the response vector of the surrogate model by  $\mathbf{R}_s(\mathbf{x}, \mathbf{t})$  and the response vector of the fine model by  $\mathbf{R}_f(\mathbf{x})$ . The mode response vectors represent  $S$ -parameters of the filter structure as a function of frequency. Here,  $\mathbf{x}$  is the design parameters vector and  $\mathbf{t}$  is the tuning parameters vector. In our case, the design parameters are geometry dimensions of the filter structure, whereas tuning variables are certain parameters of the surrogate model that are adjusted in order to reduce misalignment between the surrogate and the fine model.

The overall goal is to find

$$\mathbf{x}_{opt} = \arg \min_{\mathbf{x}} U(\mathbf{R}_f(\mathbf{x})) \quad (4)$$

where  $U$  is an objective function that encodes the design specifications. Here, we use minimax objective function [2] that determines the maximum violation of the design requirements imposed on  $S$ -parameters over frequency bands of interest.

### 3.1 Algorithm

The optimization algorithm is illustrated by a diagram in Fig. 9, and can be described as follows:

1. Set  $i = 0$  and the initial point  $\mathbf{x}^{(i)} = \mathbf{x}^{init}$ ;
2. Evaluate  $\mathbf{R}_f(\mathbf{x}^{(i)})$ ;
3. Calibrate the surrogate model by adjusting the tuning parameters  $\mathbf{t}^{(i)} = \arg \min \{t : \|\mathbf{R}_f(\mathbf{x}^{(i)}) - \mathbf{R}_s(\mathbf{x}^{(i)}, \mathbf{t})\|\}$ ;
4. Obtain the new design by optimizing the surrogate model  $\mathbf{x}^{(i+1)} = \arg \min \{\mathbf{x}, \|\mathbf{x} - \mathbf{x}^{(i)}\| \leq \delta^{(i)} : U(\mathbf{R}_s(\mathbf{x}, \mathbf{t}^{(i)}))\}$ ;
5. Evaluate the fine model  $\mathbf{R}_f(\mathbf{x}^{(i+1)})$ ;
6. If the termination conditions are not satisfied, set  $i = i + 1$  and go to step 3; else END.

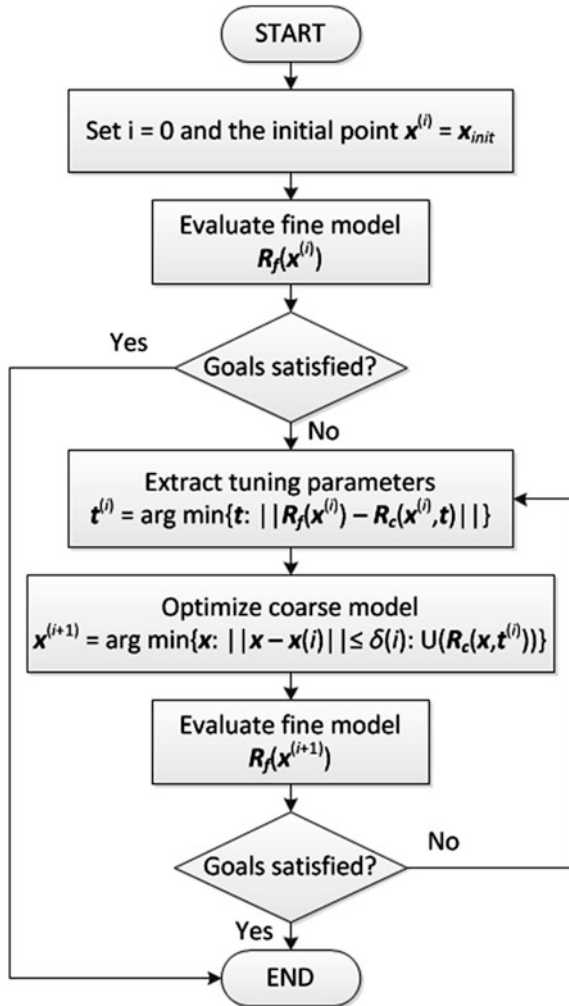
In Step 3, the parameter extraction procedure is executed that identifies the values of the tuning parameters  $\mathbf{t}$  so that the surrogate model becomes as good representation of the fine model at the current iteration point  $\mathbf{x}^{(i)}$ . As indicated in Step 4, the surrogate model optimization is embedded in the trust region (TR) framework [6] to improve convergence properties of the algorithm;  $\delta^{(i)}$  is the TR radius updated in each iteration using conventional rules [6]. The procedure is terminated if the goals are satisfied or if the predefined number of iteration exceeded.

## 4 Illustration Examples

In this section, we illustrate the design methodology introduced in this Sect. 3 using two examples of E-plane filters of the second- and the fourth order.



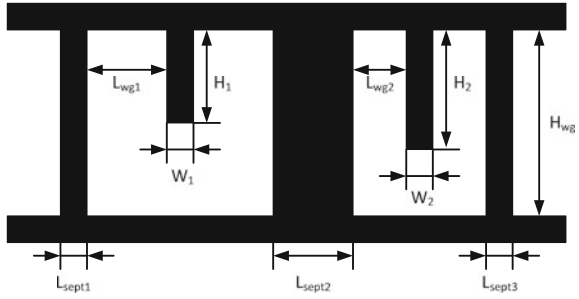
**Fig. 9** Optimization flow diagram



**4.1 Example 1: 2nd-Order Filter with Two EPS**

The models and the optimization algorithm were tested on a 2nd-order inline extracted pole bandpass filter with two symmetric EPS connected in series through a septum. Figure 10 presents the configuration of the E-plane insert for the filter. The design parameters are  $\mathbf{x} = [H_1 H_2 L_{sept1} L_{sept2} L_{sept3} L_{wg1} L_{wg2}]^T$ . Width of the fins is fixed to  $W = 2$  mm. The waveguide parameters are: width  $W_{wg} = 22.86$  mm, height  $H_{wg} = 10.16$  mm and  $\epsilon_r = 1.00059$ ; they remain constant throughout the entire optimization procedure. The corresponding specifications of the filter are given as follows:  $|S_{11}| \leq -20$  dB for  $9.92$  GHz  $\leq f \leq 10.08$  GHz, and  $|S_{21}| \leq -40$  dB for  $10.9$  GHz  $\leq f \leq 12.2$  GHz.

**Fig. 10** Configuration of the E-plane insert for the 2nd-order filter



The initial design parameters  $\mathbf{x}_{init} = [6 \ 5.5 \ 1.5 \ 6.5 \ 2 \ 1.5 \ 3]^T$  mm are found by the generalized coupling coefficients extraction technique [7], which is helpful at attaining a good initial design.

The tuning parameters  $\mathbf{t} = [k_1 \ k_2 \ k_3 \ k_4 \ c_1 \ c_2 \ c_3 \ c_4 \ c_5 \ c_6]^T$  are obtained by fitting absolute values of the S-parameters by the least square criterion. Quality of extraction of the tuning parameters is crucial for the success of the procedure, as discrepancy between  $\mathbf{R}_s(\mathbf{x}_{init}, \mathbf{t}(0))$  and  $\mathbf{R}_s(\mathbf{x}_{init}, 0)$  is rather considerable, as illustrated in Fig. 11. On the other hand, the response  $\mathbf{R}_s(\mathbf{x}_{init}, \mathbf{t}(0))$  of the corrected surrogate is virtually indistinguishable from  $\mathbf{R}_f(\mathbf{x}_{init})$ , which indicates that the circuit model developed in Sect. 2 is a suitable tool to conduct space mapping optimization of the extracted pole filter.

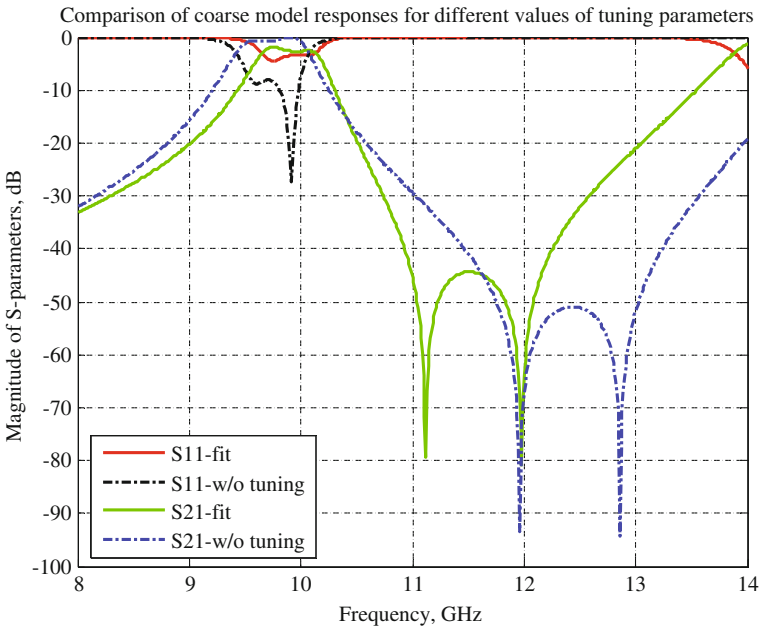


**Fig. 11** Comparison of  $\mathbf{R}_s(\mathbf{x}_{init}, \mathbf{t}(0))$  and  $\mathbf{R}_s(\mathbf{x}_{init}, 0)$ .  $\mathbf{R}_s(\mathbf{x}_{init}, \mathbf{t}(0))$  is essentially identical to fine model response at  $\mathbf{x}_{init}$

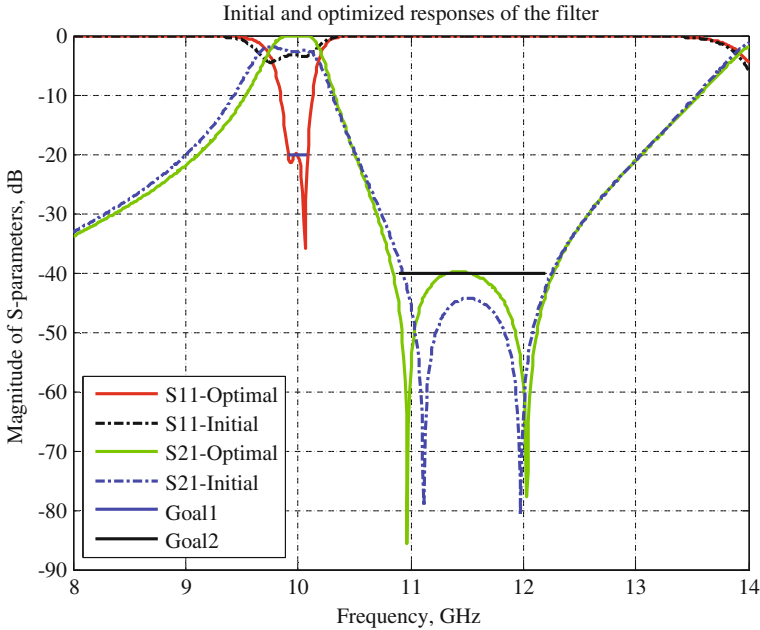


**Fig. 12** Initial and optimized responses of the 2nd-order filter

Figure 12 shows the optimal response  $\mathbf{R}_f(\mathbf{x}_{opt})$  compared to the initial  $\mathbf{R}_f(\mathbf{x}_{init})$ , where  $\mathbf{x}_{opt} = [6.09 \ 5.45 \ 1.71 \ 6.42 \ 2.09 \ 1.42 \ 2.77]^T$  mm. The optimum has been obtained for 6 iterations and 9 evaluations of the fine model.

### 4.2 Example 2: 4th-Order Filter with Three EPS

A 4th-order inline extracted pole bandpass filters with three EPS, one of which produces two poles and a zero [8], is chosen as another test example. Configuration of the E-plane waveguide insert implementing the filter is shown in Fig. 13. The filter contains three symmetric EPS: the two standard ones, as considered in Sect. 4.1, are directly coupled to input and output through a septum, while the dual-mode EPS is located between them. All the EPS are connected in series by means of septa.

The design parameters are  $\mathbf{x} = [H_1 \ H_2 \ H_3 \ L_{sept1} \ L_{sept2} \ L_{sept3} \ L_{sept4} \ L_{wg1} \ L_{wg2} \ L_{wg3} \ W_2]^T$ . Widths of the first and third fins are fixed to  $W_1 = W_3 = 1.2$  mm. The waveguide parameters are: width  $W_{wg} = 22.86$  mm, height  $H_{wg} = 10.16$  mm and  $\epsilon_r = 1.00059$ , and they remain unchanged throughout the optimization.

The corresponding specifications of the filter are given as follows:

- $|S_{11}| \leq -20$  dB for  $10.925 \text{ GHz} \leq f \leq 11.075 \text{ GHz}$ ;
- $|S_{21}| \leq -60$  dB for  $10.58 \text{ GHz} \leq f \leq 10.62 \text{ GHz}$ ;

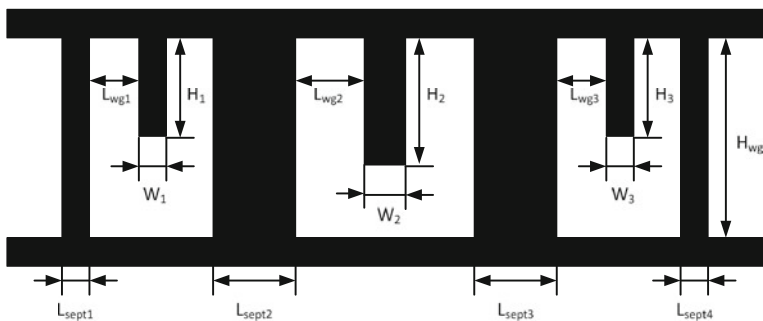


Fig. 13 Configuration of the E-plane insert for the 4th-order filter

- $|S_{21}| \leq -60$  dB for  $11.38$  GHz  $\leq f \leq 11.42$  GHz;
- $|S_{21}| \leq -70$  dB for  $11.68$  GHz  $\leq f \leq 11.72$  GHz.

The initial design parameters  $x_{init} = [6.1 \ 7.9 \ 5.85 \ 1.1 \ 10.5 \ 10.2 \ 1.4 \ 0.8 \ 12.5 \ 1.1 \ 3.5]^T$  mm are found by the generalized coupling coefficients extraction technique [7] and further tuning.

The tuning parameters  $t = [k_1 \ k_2 \ k_3 \ k_4 \ k_5 \ k_6 \ c_1 \ c_2 \ c_3 \ c_4 \ c_5 \ c_6 \ c_7 \ c_8 \ c_9 \ L_{add}]^T$  are obtained by fitting absolute values of the S-parameters by the least square criterion. Here, an additional waveguide section  $L_{add}$  has been added in series to  $L_{wg2}$  as a tuning parameter in order to improve the coarse model  $R_s(x_{init}, t(0))$  and enable fitting of the fine model response  $R_f(x_{init})$  with sufficient accuracy.

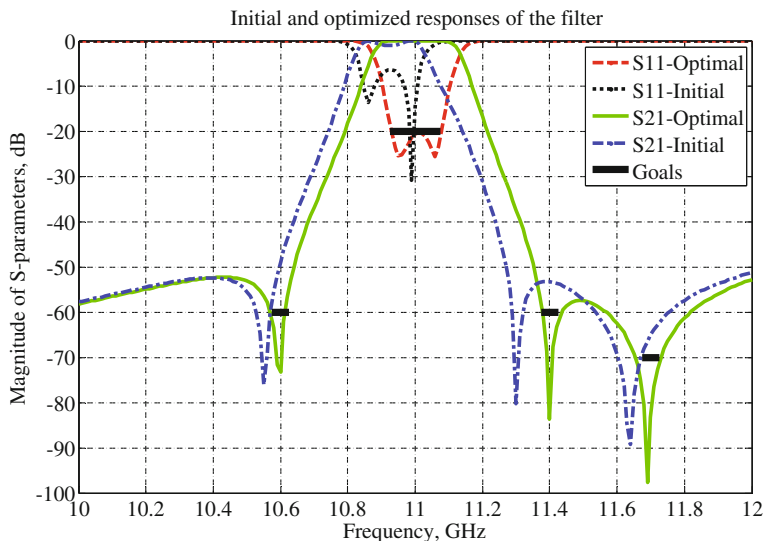


Fig. 14 Initial and optimized responses of the 4th-order filter

The optimized design has been obtained in 9 space mapping iterations with 14 evaluations of the fine model. The optimal response  $\mathbf{R}_f(\mathbf{x}_{opt})$  compared to the initial  $\mathbf{R}_f(\mathbf{x}_{init})$ , where  $\mathbf{x}_{opt} = [6.05 \ 7.89 \ 5.80 \ 1.19 \ 10.31 \ 10.39 \ 1.29 \ 0.74 \ 12.30 \ 1.26 \ 3.60]^T$  mm, is shown in Fig. 14.

## 5 Conclusions

A design procedure for inline E-plane waveguide extracted pole filters that includes surrogate modeling technique of this type of structures has been presented. The solution contains novel circuit models for septa, resonating fins and coupling effects between them, and enables use of surrogate-based optimization for this class of filters. Two design examples of a 2nd-order filter with 2 EPS and a 4th-order filter with 3 EPS connected in series have been demonstrated using implicit space mapping as an optimization engine. The optimum designs have been obtained at the cost of a few EM simulations of the filter structure.

**Acknowledgments** The authors thank Computer Simulation Technology AG for making CST Microwave Studio available. This work was supported in part by the Icelandic Centre for Research (RANNIS) Grants 120016021 and 13045051.

## References

1. Agilent ADS version (2011) Agilent Technologies, Santa Clara, CA, USA
2. Bandler JW, Cheng QS, Dakrouy SA, Mohamed AS, Bakr MH, Madsen K, Sondergaard J (2004) Space mapping: the state of the art. *IEEE Trans Microwave Theory Tech* 52 (1):337–361
3. Chang K, Khan PJ (1976a) Equivalent circuit of a narrow axial strip in waveguide. *IEEE Trans Microwave Theory Tech* 24(9):611–615
4. Chang K, Khan PJ (1976b) Coupling between narrow transverse inductive strips in waveguide. *IEEE Trans Microwave Theory Tech* 24(2):101–105
5. Cheng QS, Bandler JW, Koziel S (2008) An accurate microstrip hairpin filter design using implicit space mapping. *Microwave Mag* 9(1):79–88
6. Conn AR, Gould NIM, Toint PL (2000) Trust region methods. *MPS-SIAM Series on Optimization*
7. Glubokov O, Budimir D (2011a) Extraction of generalized coupling coefficients for inline extracted pole filters with nonresonating nodes. *IEEE Trans Microwave Theory Tech* 59 (12):3023–3029
8. Glubokov O, Budimir D (2011b) Novel inline waveguide e-plane filter using dual-mode extracted pole section. In: *European microwave conference (EuMC)*, pp 99–102
9. Koziel S, Bandler JW, Madsen K (2006) Space mapping framework for engineering optimization: theory and implementation. *IEEE Trans Microwave Theory Tech* 54:3721–3730
10. Koziel S, Cheng QS, Bandler JW (2008) Space mapping. *IEEE Microwave Mag* 9(6):105–122